SUPPLEMENT: "THE RATE OF BINARY BLACK HOLE MERGERS INFERRED FROM ADVANCED LIGO OBSERVATIONS SURROUNDING GW150914" (2016, ApJL, 833, L1)

LIGO Scientific Collaboration and Virgo Collaboration
(See the end matter for the full list of authors.)

ABSTRACT

This article provides supplemental information for a Letter reporting the rate of (BBH) coalescences inferred from 16 days of coincident Advanced LIGO observations surrounding the transient (GW) signal GW150914. In that work we reported various rate estimates whose 90% confidence intervals fell in the range 2–600 Gpc^{-3} yr^{-1}. Here we give details on our method and computations, including information about our search pipelines, a derivation of our likelihood function for the analysis, a description of the astrophysical search trigger distribution expected from merging BBHs, details on our computational methods, a description of the effects and our model for calibration uncertainty, and an analytic method for estimating our detector sensitivity, which is calibrated to our measurements.

Key words: gravitational waves – stars: black holes

Supporting material: data behind figures

The first detection of a gravitational-wave (GW) signal from a merging binary black hole (BBH) system was described in Abbott et al. (2016d). Abbott et al. (2016g) reported on inference of the local BBH merger rate from surrounding Advanced LIGO observations. This Supplement provides supporting material and methodological details for Abbott et al. (2016g, hereafter referred to as the Letter).

1. SEARCH PIPELINES

Both the pycbc and gstlal pipelines are based on matched filtering against a bank of template waveforms. See Abbott et al. (2016c) for a detailed description of the pipelines in operation around the time of GW150914; here we provide an abbreviated description.

In the pycbc pipeline, the single-detector signal-to-noise ratio (S/N) is re-weighted by a chi-squared factor (Allen 2005) to account for template-data mismatch (Babak et al. 2013); the re-weighted single-detector S/Ns are combined in quadrature to produce a detection statistic for search triggers.

The gstlal pipeline's detection statistic, however, is based on a likelihood ratio (Cannon et al. 2013, 2015) constructed from the single-detector S/Ns and a signal-consistency statistic. An analytic estimate of the distribution of astrophysical signals in multiple-detector S/N and signal-consistency statistic space is compared to a measured distribution of single-detector triggers without a coincident counterpart in the other detector to form a multiple-detector likelihood ratio.

Both pipelines rely on an empirical estimate of the search background, making the assumption that triggers of terrestrial origin occur independently in the two detectors. The background estimate is built from observations of single-detector triggers over a long time (gstlal) or through searching over a data stream with one detector's output shifted in time relative to the other's by an interval that is longer than the light travel time between detectors, ensuring that no coincident astrophysical signals remain in the data (pycbc). For both pipelines it is not possible to produce an instantaneous background estimate at a particular time; this drives our choice of likelihood function, as described in Section 2.

The gstlal pipeline natively determines the functions $p_0(x)$ and $p_1(x)$ for its detection statistic x. For this analysis a threshold of $x_{\min} = 5$ was applied, which is sufficiently low that the trigger density is dominated by terrestrial triggers near a threshold. There were $M = 15\,848$ triggers observed above this threshold in the 17 days of observation time analyzed by gstlal.

For pycbc, the quantity x' is the re-weighted S/N detection statistic.[137] We set a threshold $x'_{\min} = 8$, above which $M' = 270$ triggers remain in the search. We use a histogram of triggers collected from time-shifted data to estimate the terrestrial trigger density, $p_0(x')$, and a histogram of the recovered triggers from the injection sets described in Section 2.2 of the Letter to estimate the astrophysical trigger density, $p_1(x')$. These estimates are shown in Figure 1. The uncertainty in the distribution of triggers from this estimation procedure is much smaller than the uncertainty in the overall rate from the finite number statistics (see, for example, Figure 5). The empirical estimate is necessary to properly account for the interaction of the various single- and double-interferometer thresholds in the pycbc search (Abbott et al. 2016c). At high S/N, where these thresholds are irrelevant, the astrophysical triggers follow an approximately flat-space volumetric density (see Section 3) of

$$p_1(x') \simeq \frac{3x'^3_{\min}}{x'^4},\qquad(1)$$

but they deviate from this at smaller S/N due to threshold effects in the search.

For the pycbc pipeline, a detection statistic $x' \geqslant 10.1$ corresponds to an estimated search false alarm rate (FAR) of one per century.

2. DERIVATION OF POISSON MIXTURE MODEL LIKELIHOOD

In this section we derive the likelihood function in Equation (3) of the Letter. Consider a search of the type described in

---

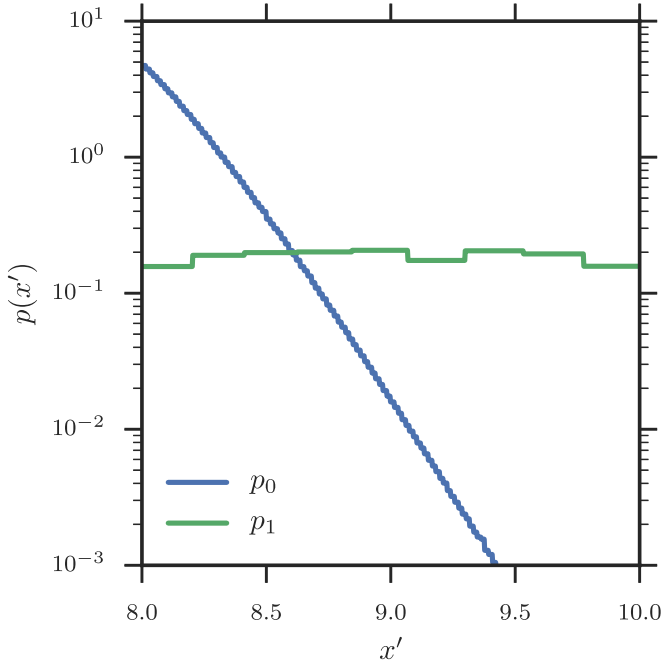[137] When quoting pipeline-specific values we distinguish pycbc quantities with a prime.

Figure 1. Inferred terrestrial (p_0; blue) and astrophysical (p_1; green) trigger densities for the `pycbc` pipeline as described in Section 1.

(The data used to create this figure are available.)

Section 1 over N_T intervals of time, of width $\delta_i, \{i = 1, \ldots, N_T\}$. Triggers above some fixed threshold occur with an instantaneous rate in time and detection statistic x given by the sum of the terrestrial and astrophysical rates:

$$\frac{dN}{dtdx}(t, x) = R_0(t)p_0(x; t) + R_1(t)V(t)p_1(x; t), \quad (2)$$

where $R_0(t)$ is the instantaneous rate (number per unit time) of terrestrial triggers, $R_1(t)$ is the instantaneous rate density (number per unit time per unit comoving volume) of astrophysical triggers, p_0 is the instantaneous density in the detection statistic of terrestrial triggers, p_1 is the instantaneous density in the detection statistic of astrophysical triggers, and $V(t)$ is the instantaneous sensitive comoving redshifted volume (Abbott et al. 2016a; see also Equation (15) of the Letter) of the detectors to the assumed source population. The astrophysical rate R_1 is to any reasonable approximation constant over our observations so we will drop the time dependence of this term from here on.[138] Note that R_0 and R_1 have different units in this expression; the former is a rate (per time), while the latter is a rate density (per time-volume). The density p_1 is independent of source parameters as described in Section 3. Let

$$\frac{dN}{dt} \equiv \int dx \frac{dN}{dtdx} = R_0(t) + R_1V(t). \quad (3)$$

If the search intervals δ_i are sufficiently short, they will contain at most one trigger and the time-dependent terms in Equation (2) will be approximately constant. Then the likelihood for a set of times and detection statistics of triggers, $\{(t_j, x_j)|j = 1, \ldots, M\}$, is a product over intervals containing a trigger (indexed by j) and intervals that do not contain a trigger

(indexed by k) of the corresponding Poisson likelihoods

$$\mathcal{L} = \left\{ \prod_{j=1}^{M} \frac{dN}{dtdx}(t_j, x_j) \exp\left[-\delta_j \frac{dN}{dt}(t_j) \right] \right\}$$
$$\times \left\{ \prod_{k=1}^{N_T - M} \exp\left[-\delta_k \frac{dN}{dt}(t_k) \right] \right\} \quad (4)$$

(see Farr et al. 2015, Equation (21), or Loredo & Wasserman 1995 Equation (2.8)).[139] Now let the width of the observation intervals δ_i go to zero uniformly as the number of intervals goes to infinity. Then the products of exponentials in Equation (4) become an exponential of an integral, and we have

$$\mathcal{L} = \prod_{j=1}^{M} \left[\frac{dN}{dtdx}(t_j, x_j) \right] \exp[-N], \quad (5)$$

where

$$N = \int dt \frac{dN}{dt} \quad (6)$$

is the expected number of triggers of both types in the total observation time T.

As discussed in Section 1, in our search we observe that R_0 remains approximately constant and that p_0 retains its shape over the observation time discussed here; this assumption is used in our search background estimation procedure (Abbott et al. 2016c). The astrophysical distribution of triggers is universal (Section 3) and also time-independent. Finally, the detector sensitivity is observed to be stable over our 16 days of coincident observations, so $V(t) \simeq$ const (Abbott et al. 2016b). We therefore choose to simply ignore the time dimension in our trigger set. This generates an estimate of the rate that is sub-optimal (i.e., has larger uncertainty) but consistent with using the full data set to the extent that the detector sensitivity varies in time; since this variation is small, the loss of information about the rate will be correspondingly small. We *do* capture any variation in the sensitivity with time in our Monte Carlo procedure for estimating $\langle VT \rangle$, which is described in Section 2.2 of the Letter.

If we ignore the trigger time, then the appropriate likelihood to use is a marginalization of Equation (5) over the t_j. Let

$$\bar{\mathcal{L}} \equiv \int [\prod_j dt_j] \mathcal{L}$$
$$= \prod_j [\Lambda_0 p_0(x_j) + \Lambda_1 p_1(x_j)] \exp[-\Lambda_0 - \Lambda_1], \quad (7)$$

where

$$\Lambda_0 p_0(x) = \int dt \, R_0(t) p_0(x; t), \quad (8)$$

and

$$\Lambda_1 p_1(x) = \int dt \, R_1 V(t) p_1(x; t), \quad (9)$$

with

$$\int dx \, p_0(x) = \int dx \, p_1(x) = 1. \quad (10)$$

---

[138] The astrophysical rate can, in principle, also depend on redshift, but in this paper we assume that the BBH coalescence rate is constant in the comoving frame.

[139] There is a typo in Equation (2.8) of Loredo & Wasserman (1995). The second term in the final bracket is missing a factor of δt.
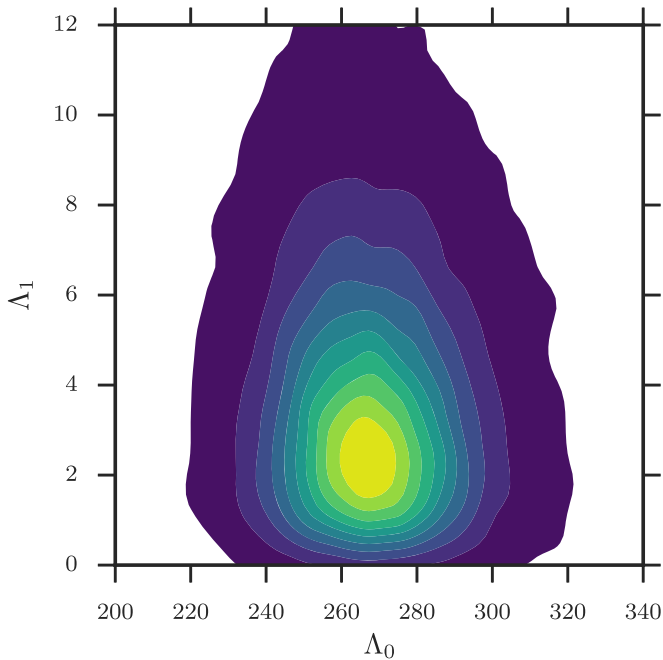
Figure 2. Two-dimensional posterior on terrestrial and astrophysical trigger expected counts (Λ_0 and Λ_1 in Equation (5) of the Letter) for the pycbc search. Contours are drawn at the 10%, 20%, …, 90%, and 99% credible levels. There is no meaningful correlation between the two variables. The Poisson uncertainty in the terrestrial count is $\sim \sqrt{270}$, or 16, which is also very near the Poisson uncertainty in the total count. Because this uncertainty is much larger than the astrophysical count, changes in the astrophysical count do not force the terrestrial count to adjust in a meaningful way and the variables are uncorrelated in the posterior.

(The data used to create this figure are available.)

If we assume that R_1 is constant in (comoving) time, and measure $p_1(x)$ by accumulating recovered injections throughout the run as we have done, then this expression reduces to the likelihood in Equation (3) of the Letter. A similar argument with an additional population of triggers produces Equation (10) of the Letter.

2.1. The Expected Number of Background Triggers

The procedure for estimating $p_0(x)$ in the pycbc pipeline also provides an estimate of the mean number of background events per experiment Λ_0 (Abbott et al. 2016c). The procedure for estimating p_0 used in the gstlal pipeline, however, does not naturally provide an estimate of Λ_0; instead gstlal estimates Λ_0 by fitting the observed number of triggers to a Poisson distribution. We have chosen to leave Λ_0 as a free parameter in our canonical analysis with a broad prior and infer it from the observed data, rather than using the pycbc background estimate to constrain the prior, which would result in a much narrower posterior on Λ_0. This is equivalent to the gstlal procedure for Λ_0 estimation in the absence of signals; the presence of a small number of signals in our data here does not substantially change the Λ_0 estimate due to the overwhelming number of background triggers in the data set.

Using a broad prior on Λ_0 is conservative in the sense that it will broaden the posterior on Λ_1 from which we infer rates. However, because there are so many more triggers in searches of terrestrial origin than there are in those of astrophysical origin there is little correlation between Λ_0 and Λ_1, so there is

little difference between the posterior we obtain on Λ_1 and the posterior we would have obtained had we implemented the tight prior on Λ_0. Figure 2 shows the two-dimensional posterior we obtain from Equation (5) of the Letter on Λ_0 and Λ_1.

We have checked that using a δ-function prior

$$p(\Lambda_0) = \delta(\Lambda_0 - 270) \qquad (11)$$

in the pycbc analysis that is the result of the pipeline Λ_0 estimate from timeslides[140] (Abbott et al. 2016c) and using a looser prior that is the result of a gstlal estimate on a single set of time-slid data produce no meaningful change in our results. Figure 3 shows our canonical rate posterior inferred with the pycbc Λ_0 prior in Equation (11) and our canonical broad prior.

3. UNIVERSAL ASTROPHYSICAL TRIGGER DISTRIBUTION

Both the pycbc and gstlal pipelines rely on the S/N as part of their detection statistic, x. The S/N of an astrophysical trigger is a function of the detector noise at the time of detection and the parameters of the trigger. Schutz (2011) and Chen & Holz (2014) demonstrate that the distribution of the expected S/N $\langle\rho\rangle$ in a simple model of a detection pipeline that simply thresholds on S/N, $\rho \geqslant \rho_{th}$, with sources in the local universe is *universal*, that is, independent of the source properties. It follows

$$p(\langle\rho\rangle) = \frac{3\rho_{th}^3}{\langle\rho\rangle^4}. \qquad (12)$$

This result follows from the fact that the expected value of the S/N in a matched-filter search for compact binary coalescence (CBC) signals scales inversely with transverse comoving distance (Hogg 1999):

$$\langle\rho\rangle = \frac{A(m_1, m_2, \boldsymbol{a}_1, \boldsymbol{a}_2, S(f), z)B(\text{angles})}{D_M}, \qquad (13)$$

where A is an amplitude factor that depends on the intrinsic properties (source-frame masses and spins) of the source, the detector sensitivity expressed as a noise power spectral density $S(f)$ as a function of observer frequency and redshift z, and B is an angular factor depending on the location of the source in the sky and the relative orientations of the binary orbit and detector. The redshift enters A only through shifting the source waveform to lower frequency at higher redshift, changing A because the sensitivity varies with observer frequency f. For the redshifts to which we are sensitive to BBH in this observation period this effect on A is small.

If we assume that the distribution of source parameters is constant over the range of distances to which we are sensitive, and ignore the small redshift-dependent sensitivity correction mentioned above, then the distribution of S/N will be governed entirely by the distribution of distances of the sources, which, in the local universe, is approximately

$$p(D_M) \propto D_M^2, \qquad (14)$$

yielding the distribution of S/N given in Equation (12).

---

[140] While the statistical uncertainty on the pipeline Λ_0 estimate is not precisely zero, $\sigma_{\Lambda_0}/\Lambda_0 \lesssim 10^{-3}$, it is so small that a δ-function prior is appropriate.
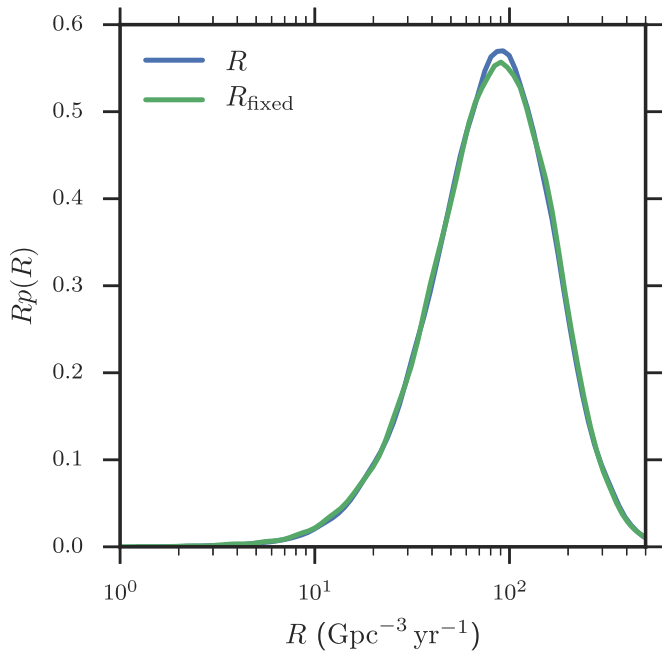
Figure 3. Posterior on the population-based rate obtained from our canonical analysis (blue) and an analysis where the expected background count, Λ_0, is fixed to the value measured by the `pycbc` pipeline, $\Lambda_0 = 270$ (green). There is no meaningful change in the rate posterior between the two analyses.
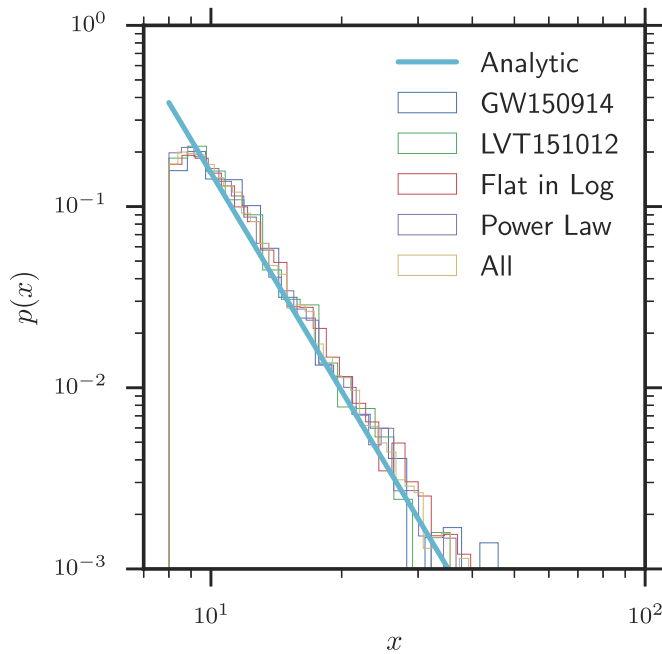
(The data used to create this figure are available.)

Figure 4. Distribution of detection statistics in the `pycbc` pipeline for the signals recovered in the injection campaigns used to estimate sensitive time-volumes for various BBH population assumptions (see Sections 2 and 3 of the Letter). The solid line gives the analytic approximation to the distribution from Equation (12), which agrees well with the recovered statistics for loud signals; for quieter signals the interaction of various thresholds in the pipeline causes the distribution to deviate from the analytic approximation, but it remains independent of the source distribution.

(The data used to create this figure are available.)

Both the `pycbc` and `gstlal` pipelines use goodness-of-fit statistics in addition to S/N and employ a more complicated system of thresholds than this simple model, but the empirical distribution of detection statistics remains, to an approximation

suitable for our purposes, independent of the source parameters. Figure 4 shows the distribution of recovered detection statistics for the various injection campaigns with varying source distribution used to estimate sensitive time-volumes in the `pycbc` pipeline. In each injection campaign $\mathcal{O}(1000)$ signals were recovered. For loud signals, the detection statistic is proportional to S/N in this pipeline, and the distribution is not sensitive to the complicated thresholding in the pipeline, so we recover Equation (12); for quiet signals the interaction of various single-detector thresholds in the pipeline causes the distribution to deviate from this analytic approximation, but it remains independent of the distribution of sources. Note that the empirical distribution of detection statistics, not the analytic one, forms the basis for p_1, the foreground distribution used in this rate estimation work.

To quantify the deviations from universality, we have preformed two-sample Kolmogorov-Smirnov (KS) tests between all six pairings of the sets of detections statistics recovered in the injection campaigns described in Sections 2 and 3 of the Letter and featured in Figure 4. The most extreme KS p-value occurred with the comparison between the injection set with BBH masses drawn flat in $\log m$ and the one with masses drawn from a power law (both described in Section 3 of the Letter); this test gave a p-value of 0.013. Given that we have performed six identical comparisons we cannot reject the null hypothesis that the empirical distributions used for rate estimation from the `pycbc` pipeline are identical even at the relatively weak significance $\alpha = 0.05$. Certainly any differences in detection statistic distribution attributable to the BBH population are far too small to matter with the few astrophysical signals in our data set (compared with $\mathcal{O}(1000)$ recovered injections in each campaign).

Because the distribution of detection statistics is, to a very good approximation, *universal*, we cannot learn anything about the source population from the detection statistic alone; we must instead resort to parameter estimation (PE) follow-up (Veitch et al. 2015; Abbott et al. 2016e) of triggers to determine their parameters. The parameters of the waveform template that produced the trigger can be used to guess the parameters of the source that generated that trigger, but the bias and uncertainty in this estimate are very large compared to the PE estimate. We therefore ignore the parameters of the waveform template that generated the trigger in the assignment of triggers to BBH classes.

4. COUNT POSTERIOR

We impose a prior on the Λ parameters of:

$$p(\Lambda_1, \Lambda_0) \propto \frac{1}{\sqrt{\Lambda_1}} \frac{1}{\sqrt{\Lambda_0}}. \quad (15)$$

The posterior on expected counts is proportional to the product of the likelihood from Equation (3) of the Letter and the prior from Equation (15):

$$p(\Lambda_1, \Lambda_0 | \{x_j | j = 1, ..., M\})$$

$$\propto \left\{ \prod_{j=1}^{M} [\Lambda_1 p_1(x_j) + \Lambda_0 p_0(x_j)] \right\}$$

$$\times \exp[-\Lambda_1 - \Lambda_0] \frac{1}{\sqrt{\Lambda_1 \Lambda_0}}. \quad (16)$$

For estimation of the Poisson rate parameter in a simple Poisson model, the Jeffreys prior is $1/\sqrt{\Lambda}$. With this prior, the
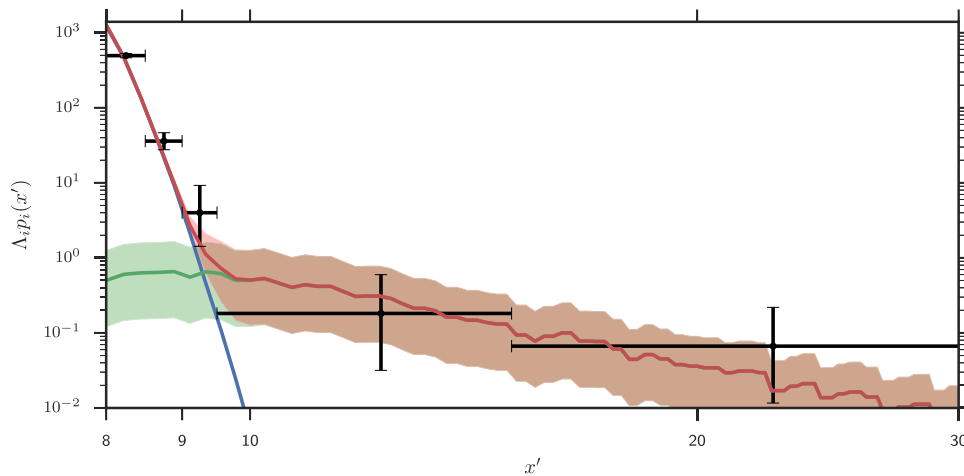
Figure 5. Inferred number density of astrophysical (green), terrestrial (blue), and all (red) triggers as a function of x' for the `pycbc` search (see Equation (1) of the Letter), using the models for each population described in Section 2.1 of the Letter. The solid lines give the posterior median and the shaded regions give the symmetric 90% credible interval from the posterior in Equation (5) of the Letter. We also show a binned estimate of the trigger number density from the search (black); bars indicate the 68% confidence Poisson uncertainty on the number of triggers in the vertical-direction and bin width in the horizontal-direction.

(The data used to create this figure are available.)

posterior mean on Λ is $N + 1/2$ for N observed counts. With a prior proportional to $1/\Lambda$ the mean is N for $N > 0$, but the posterior is improper when $N = 0$. For a flat prior, the mean is $N + 1$. Though the behavior of the mean is not identical with our mixture model posterior, it is similar; because we find $\langle \Lambda_1 \rangle \gg 1/2$, the choice of prior among these three reasonable options has little influence on our results here.

For the `pycbc` data set we find the posterior median and 90% credible range $\Lambda_1 = 3.2^{+4.9}_{-2.4}$ above our threshold. For the `gstlal` set we find the posterior median and 90% credible range $\Lambda_1 = 4.8^{+7.9}_{-3.8}$. Though we have only one event (GW150914) at exceptionally high significance, and one other at marginal significance (LVT151012), the counting analysis shows these to be consistent with the possible presence of several more events of astrophysical origin at a lower detection statistic in both pipelines.

The thresholds applied to the `pycbc` and `gstlal` triggers for this analysis are not equivalent to each other in terms of either S/N or FAR; instead, both thresholds have been chosen so that the rate of triggers of terrestrial origin ($\Lambda_0 p_0$) dominates near the threshold. Since the threshold is set at *different* values for each pipeline, we do not expect the counts to be the same between pipelines.

The estimated astrophysical and terrestrial trigger rate densities (Equation (1) of the Letter) for `pycbc` are plotted in Figure 5. We select triggers from a subset of the search parameter space (i.e., our bank of template waveforms) that contains GW150914 as well as the mass range considered for possible alternative populations of BBH binaries in Section 3 of the Letter. There are $M' = 270$ two-detector coincident triggers in this range in the `pycbc` search (Abbott et al. 2016c). Figure 5 also shows an estimate of the density of triggers that comprise our data set, which agrees well with our inference of the trigger rate.

Based on the probability of astrophysical origin inferred for LVT151012 from the two-component mixture model in Equation (16) and shown in Figure 6, we introduce a third class of signals and use a three-component mixture model with expected counts Λ_0 (terrestrial), Λ_1 (GW150914-like), and Λ_2 (LVT151012-like) to infer rates in Sections 2.1 and 2.2 of the Letter.

We use the Stan and `emcee` Markov Chain Monte Carlo samplers (Foreman-Mackey et al. 2013; Stan Development Team 2015a, 2015b) to draw samples from the posterior in Equation (5) of the Letter for the two pipelines. We have assessed the convergence and mixing of our chains using empirical estimates of the autocorrelation length in each parameter (Sokal 1996), the Gelman-Rubin R convergence statistic (Gelman & Rubin 1992), and through visual inspection of chain plots. By all measures, the chains appear to be well-converged to the posterior distribution.

Table 1 contains the full results on expected counts and associated sensitive time-volumes for both pipelines.

5. CALIBRATION UNCERTAINTY

The LIGO detectors are subject to uncertainty in their calibration, in both the measured amplitude and the phase of the GW strain. Abbott et al. (2016b) discussed the methods used to calibrate the strain output of the detector during the 16 days of coincident observations discussed here. Abbott et al. (2016b) estimated that the reported strain is accurate to within 10% in amplitude and 10 degrees in phase between 20 Hz and 1 kHz throughout the observations.

The S/Ns reported by our searches are quadratically sensitive to calibration errors because they are maximized over arrival time, waveform phase, and a template bank of waveforms (Allen 1996; Brown & LIGO Scientific Collaboration 2004). Abbott et al. (2016c) demonstrated that the other search pipeline outputs are also not affected to a significant degree by the calibration uncertainty present during our observing run. Therefore, we ignore the effects of calibration on the pipeline detection statistics x and x' that we use here to estimate rates from the `pycbc` and `gstlal` pipelines.

The amplitude calibration uncertainty in the detector results, at leading order, in a corresponding uncertainty between the luminosity distances of sources measured from real detector outputs (Abbott et al. 2016e) and the luminosity distances used to produce injected waveforms used to estimate sensitive time-volumes in this work. A 10% uncertainty in d_L at these redshifts corresponds to an approximately 30% uncertainty in volume. We model this uncertainty by treating $\langle VT \rangle$ as a
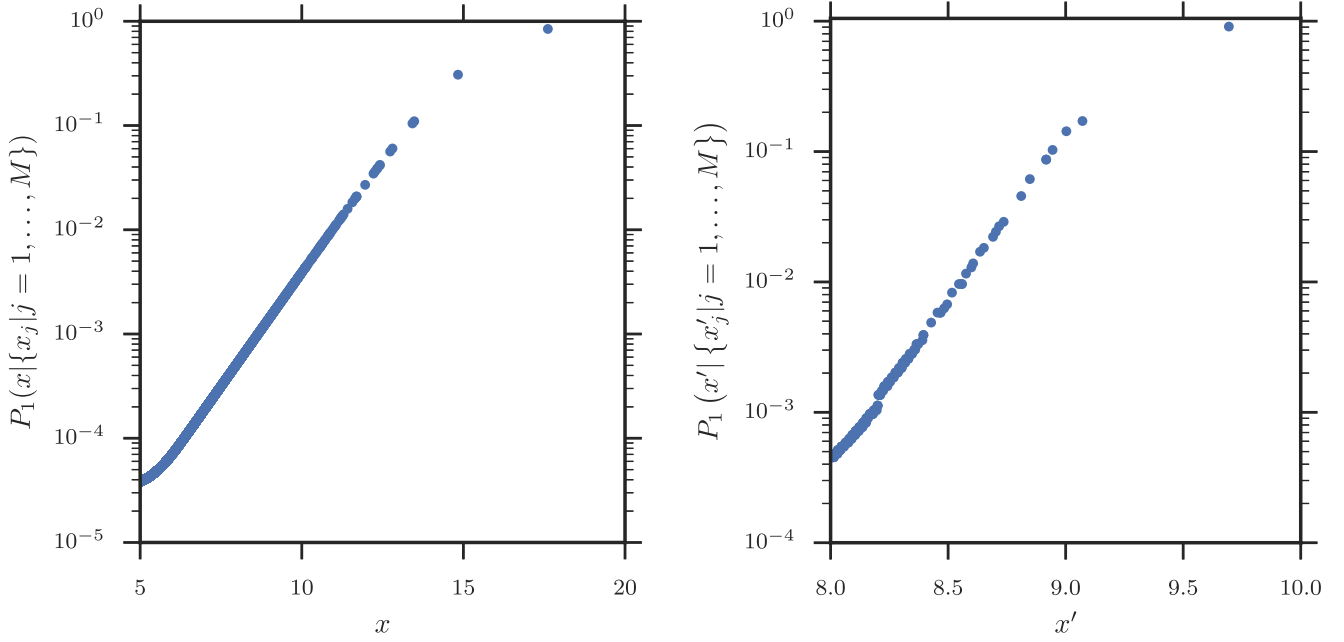
Figure 6. Posterior probability that coincident triggers in our analysis come from an astrophysical source (see Equation (7) of the Letter), taking into account the astrophysical and terrestrial expected counts estimated in Section 2.1 of the Letter. Left: the `gstlal` triggers with $x > 5$; right: `pycbc` triggers with $x' > 8$. GW150914 is not shown in the plot because its probability of astrophysical origin is effectively 100%. The only two triggers with $P_1 \gtrsim 50\%$ are GW150914 and LVT151012. For GW150914, we find $P_1 = 1$ to very high precision; for LVT151012, the `gstlal` pipeline finds $P_1 = 0.84$ and the `pycbc` pipeline finds $P_1 = 0.91$.

(The data used to create this figure are available.)

Table 1
Expected Counts and Sensitive Time-volumes to BBH Mergers Estimated under Various Assumptions

| | Λ | | $\langle VT \rangle / \mathrm{Gpc}^3\,\mathrm{yr}$ | |
	pycbc	gstlal	pycbc	gstlal
GW150914	$2.1^{+4.1}_{-1.7}$	$3.6^{+6.9}_{-2.9}$	$0.130^{+0.084}_{-0.051}$	$0.21^{+0.14}_{-0.08}$
LVT151012	$2.0^{+4.0}_{-1.7}$	$3.0^{+6.8}_{-2.7}$	$0.032^{+0.020}_{-0.012}$	$0.048^{+0.031}_{-0.019}$
Both	$4.5^{+5.5}_{-3.1}$	$7.4^{+9.2}_{-5.1}$	...	...
Astrophysical				
Flat in log mass	$3.2^{+4.9}_{-2.4}$	$4.8^{+7.9}_{-3.8}$	$0.050^{+0.032}_{-0.019}$	$0.080^{+0.051}_{-0.031}$
Power Law (-2.35)			$0.0154^{+0.0098}_{-0.0060}$	$0.024^{+0.015}_{-0.009}$

Note. See Sections 2.1, 2.2, 3, and 4 of the Letter.

parameter in our analysis, and imposing a log-normal prior:

$$p(\log \langle VT \rangle) \propto N\left(\log \mu, \frac{\sigma}{\mu}\right), \qquad (17)$$

where μ is the Monte Carlo estimate of sensitive time-volume produced from the injection campaigns described in Section 2.2 of the Letter and

$$\sigma^2 = \sigma_{\mathrm{cal}}^2 + \sigma_{\mathrm{stat}}^2, \qquad (18)$$

with $\sigma_{\mathrm{cal}} = 0.3\mu$ and σ_{stat} is the estimate of the Monte Carlo uncertainty from the finite number of recovered injections reported above. In all cases $\sigma_{\mathrm{cal}} \gg \sigma_{\mathrm{stat}}$.

Since the likelihood in Equations (3) or (10) of the Letter does not constrain $\langle VT \rangle$ independently of R, sampling over $\langle VT \rangle$ at the same time as Λ and R has the effect of convolving the log-normal distribution of $\langle VT \rangle$ with the posterior on Λ in the inference of R.
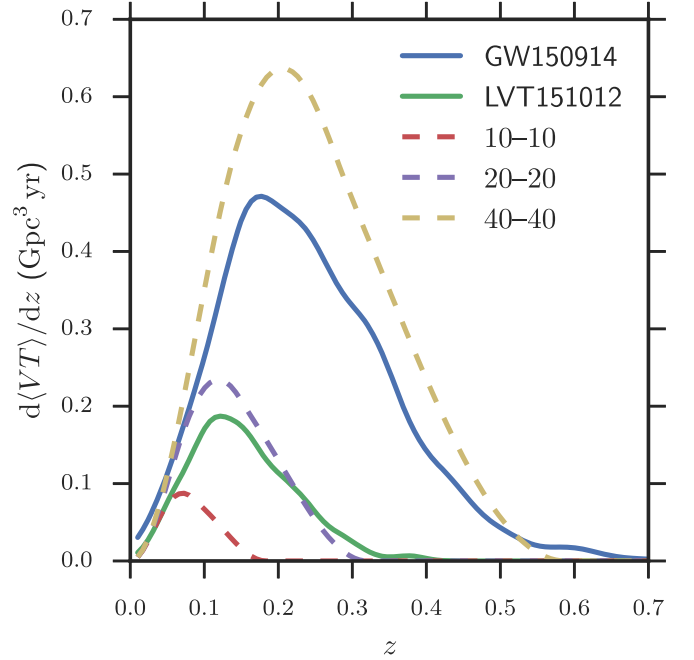

Figure 7. Rate at which sensitive time-volume accumulates with redshift. Curves labeled by component masses in $M_\odot$ are computed using the approximate prescription described in Section 6, assuming sources with fixed masses in the comoving frame and without spin; the GW150914 and LVT151012 curves are determined from the Monte Carlo injection campaign described in Section 2.2 of the Letter.

(The data used to create this figure are available.)

In spite of the 30% relative uncertainty in $\langle VT \rangle$ from calibration uncertainty, the counting uncertainty on R from the small number of detected events dominates the width of the posterior on R.

6. ANALYTIC SENSITIVITY ESTIMATE

As a rough check on our $\langle VT \rangle$ estimates and the integrand $d\langle VT \rangle/dz$, we find that the following approximate, analytic procedure also produces a good approximation to the pycbc Monte Carlo estimate in Table 1.

1. Generate inspiral–merger–ringdown waveforms in a single detector at various redshifts from the source distribution $s(\theta)$ with random orientations and sky positions.
2. Using the high-sensitivity early Advanced LIGO noise power spectral density from Abbott et al. (2016f), compute the S/N in a single detector.
3. Consider a signal found if the S/N is greater than 8.

Employed with the source distributions described above, this approximate procedure yields $\langle VT \rangle_1 \simeq 0.107 \; \text{Gpc}^3 \; \text{yr}$ and $\langle VT \rangle_2 \simeq 0.0225 \; \text{Gpc}^3 \; \text{yr}$ for the sensitivity to the two classes of merging BBH system. Figure 7 shows the sensitive time-volume integrand,

$$\frac{d\langle VT \rangle}{dz} \equiv T \frac{1}{1+z} \frac{dV_c}{dz} \int d\theta \; s(\theta) f(z, \theta), \qquad (19)$$

estimated from this procedure for systems with various parameters superimposed on the Monte Carlo estimates from the injection campaign described above.

REFERENCES

Abbott, B. P., Abbott, R., Abbott, T. D., et al. 2016a, ApJL, 818, L22
Abbott, B. P., Abbott, R., Abbott, T. D., et al. 2016b, arXiv:1602.03845
Abbott, B. P., Abbott, R., Abbott, T. D., et al. 2016c, PhRvD, 93, 122003
Abbott, B. P., Abbott, R., Abbott, T. D., et al. 2016d, PhRvL, 116, 061102
Abbott, B. P., Abbott, R., Abbott, T. D., et al. 2016e, PhRvL, 116, 241102
Abbott, B. P., Abbott, R., Abbott, T. D., et al. 2016f, LRR, 19, 1
Abbott, B. P., Abbott, R., Abbott, T. D., et al. 2016g, ApJL, 833, L1
Allen, B. 1996, LIGO Calibration Accuracy, Tech. Rep. LIGO-T960189-00-E, https://dcc.ligo.org/LIGO-T960189/public
Allen, B. 2005, PhRvD, 71, 062001
Babak, S., Biswas, R., Brady, P., et al. 2013, PhRvD, 87, 024033
Brown, D. A. & LIGO Scientific Collaboration 2004, CQGra, 21, S797
Cannon, K., Hanna, C., & Keppel, D. 2013, PhRvD, 88, 024025
Cannon, K., Hanna, C., & Peoples, J. 2015, arXiv:1504.04632
Chen, H.-Y., & Holz, D. E. 2014, arXiv:1409.0522
Farr, W. M., Gair, J. R., Mandel, I., & Cutler, C. 2015, PhRvD, 91, 023005
Foreman-Mackey, D., Hogg, D. W., Lang, D., & Goodman, J. 2013, PASP, 125, 306
Gelman, A., & Rubin, D. B. 1992, StaSc, 7, 457
Hogg, D. W. 1999, arXiv:astro-ph/9905116
Loredo, T. J., & Wasserman, I. M. 1995, ApJS, 96, 261
Schutz, B. F. 2011, CQGra, 28, 125023
Sokal, A. D. 1996, Monte Carlo Methods in Statistical Mechanics: Foundations and New Algorithms, Lecture Notes from the Cargése Summer School on "Functional Integration: Basics and Applications," http://www.stat.unc.edu/faculty/cji/Sokal.pdf
Stan Development Team 2015a, PyStan: the Python interface to Stan, Version 2.7.0, http://mc-stan.org/documentation/
Stan Development Team 2015b, Stan: A C++ Library for Probability and Sampling, Version 2.8.0, http://mc-stan.org/documentation/
Veitch, J., Raymond, V., Farr, B., et al. 2015, PhRvD, 91, 042003

AUTHORS

B. P. Abbott[1], R. Abbott[1], T. D. Abbott[2], M. R. Abernathy[1], F. Acernese[3,4], K. Ackley[5], C. Adams[6], T. Adams[7], P. Addesso[3], R. X. Adhikari[1], V. B. Adya[8], C. Affeldt[8], M. Agathos[9], K. Agatsuma[9], N. Aggarwal[10], O. D. Aguiar[11], L. Aiello[12,13], A. Ain[14], P. Ajith[15], B. Allen[8,16,17], A. Allocca[18,19], P. A. Altin[20], S. B. Anderson[1], W. G. Anderson[16], K. Arai[1], M. C. Araya[1], C. C. Arceneaux[21], J. S. Areeda[22], N. Arnaud[23], K. G. Arun[24], S. Ascenzi[13,25], G. Ashton[26], M. Ast[27], S. M. Aston[6], P. Astone[28], P. Aufmuth[8], C. Aulbert[8], S. Babak[29], P. Bacon[30], M. K. M. Bader[9], P. T. Baker[31], F. Baldaccini[32,33], G. Ballardin[34], S. W. Ballmer[35], J. C. Barayoga[1], S. E. Barclay[36], B. C. Barish[1], D. Barker[37], F. Barone[3,4], B. Barr[36], L. Barsotti[10], M. Barsuglia[30], D. Barta[38], J. Bartlett[37], I. Bartos[39], R. Bassiri[40], A. Basti[18,19], J. C. Batch[37], C. Baune[8], V. Bavigadda[34], M. Bazzan[41,42], B. Behnke[29], M. Bejger[43], A. S. Bell[36], C. J. Bell[36], B. K. Berger[1], J. Bergman[37], G. Bergmann[8], C. P. L. Berry[44], D. Bersanetti[45,46], A. Bertolini[9], J. Betzwieser[6],

S. Bhagwat[35], R. Bhandare[47], I. A. Bilenko[48], G. Billingsley[1], J. Birch[6], R. Birney[49], S. Biscans[10], A. Bisht[8,17], M. Bitossi[34], C. Biwer[35], M. A. Bizouard[23], J. K. Blackburn[1], C. D. Blair[50], D. G. Blair[50], R. M. Blair[37], S. Bloemen[51], O. Bock[8], T. P. Bodiya[10], M. Boer[52], G. Bogaert[52], C. Bogan[8], A. Bohe[29], P. Bojtos[53], C. Bond[44], F. Bondu[54], R. Bonnand[7], B. A. Boom[9], R. Bork[1], V. Boschi[18,19], S. Bose[14,55], Y. Bouffanais[30], A. Bozzi[34], C. Bradaschia[19], P. R. Brady[16], V. B. Braginsky[48], M. Branchesi[56,57], J. E. Brau[58], T. Briant[59], A. Brillet[52], M. Brinkmann[8], V. Brisson[23], P. Brockill[16], A. F. Brooks[1], D. A. Brown[35], D. D. Brown[44], N. M. Brown[10], C. C. Buchanan[2], A. Buikema[10], T. Bulik[60], H. J. Bulten[9,61], A. Buonanno[29,62], D. Buskulic[7], C. Buy[30], R. L. Byer[40], L. Cadonati[63], G. Cagnoli[64,65], C. Cahillane[1], J. Calderón Bustillo[63,66], T. Callister[1], E. Calloni[4,67], J. B. Camp[68], K. C. Cannon[69], J. Cao[70], C. D. Capano[8], E. Capocasa[30], F. Carbognani[34], S. Caride[71], J. Casanueva Diaz[23], C. Casentini[25,13], S. Caudill[16], M. Cavaglià[21], F. Cavalier[23], R. Cavalieri[34], G. Cella[19], C. B. Cepeda[1], L. Cerboni Baiardi[56,57], G. Cerretani[18,19], E. Cesarini[13,25], R. Chakraborty[1], T. Chalermsongsak[1], S. J. Chamberlin[72], M. Chan[36], S. Chao[73], P. Charlton[74], E. Chassande-Mottin[30], H. Y. Chen[75], Y. Chen[76], C. Cheng[73], A. Chincarini[46], A. Chiummo[34], H. S. Cho[77], M. Cho[62], J. H. Chow[20], N. Christensen[78], Q. Chu[50], S. Chua[59], S. Chung[50], G. Ciani[5], F. Clara[37], J. A. Clark[63], F. Cleva[52], E. Coccia[12,13,25], P.-F. Cohadon[59], A. Colla[28,79], C. G. Collette[80], L. Cominsky[81], M. Constancio, Jr.[11], A. Conte[28,79], L. Conti[42], D. Cook[37], T. R. Corbitt[2], N. Cornish[31], A. Corsi[71], S. Cortese[34], C. A. Costa[11], M. W. Coughlin[78], S. B. Coughlin[82], J.-P. Coulon[52], S. T. Countryman[39], P. Couvares[1], E. E. Cowan[63], D. M. Coward[50], M. J. Cowart[6], D. C. Coyne[1], R. Coyne[71], K. Craig[36], J. D. E. Creighton[16], J. Cripe[2], S. G. Crowder[83], A. Cumming[36], L. Cunningham[36], E. Cuoco[34], T. Dal Canton[8], S. L. Danilishin[36], S. D'Antonio[13], K. Danzmann[8,17], N. S. Darman[84], V. Dattilo[34], I. Dave[47], H. P. Daveloza[85], M. Davier[23], G. S. Davies[36], E. J. Daw[86], R. Day[34], S. De[35], D. DeBra[40], G. Debreczeni[38], J. Degallaix[65], M. De Laurentis[4,67], S. Deléglise[59], W. Del Pozzo[44], T. Denker[8,17], T. Dent[8], H. Dereli[52], V. Dergachev[1], R. De Rosa[4,67], R. T. DeRosa[6], R. DeSalvo[87,88], S. Dhurandhar[14], M. C. Díaz[85], L. Di Fiore[4], M. Di Giovanni[28,79], A. Di Lieto[18,19], S. Di Pace[28,79], I. Di Palma[8,29], A. Di Virgilio[19], G. Dojcinoski[89], V. Dolique[65], F. Donovan[10], K. L. Dooley[21], S. Doravari[6,8], R. Douglas[36], T. P. Downes[16], M. Drago[8,90,91], R. W. P. Drever[1], J. C. Driggers[37], Z. Du[70], M. Ducrot[7], S. E. Dwyer[37], T. B. Edo[86], M. C. Edwards[78], A. Effler[6], H.-B. Eggenstein[8], P. Ehrens[1], J. Eichholz[5], S. S. Eikenberry[5], W. Engels[76], R. C. Essick[10], T. Etzel[1], M. Evans[10], T. M. Evans[6], R. Everett[72], M. Factourovich[39], V. Fafone[12,13,25], H. Fair[35], S. Fairhurst[92], X. Fan[70], Q. Fang[50], S. Farinon[46], B. Farr[75], W. M. Farr[44], M. Favata[89], M. Fays[92], H. Fehrmann[8], M. M. Fejer[40], I. Ferrante[18,19], E. C. Ferreira[11], F. Ferrini[34], F. Fidecaro[18,19], I. Fiori[34], D. Fiorucci[30], R. P. Fisher[35], R. Flaminio[65,93], M. Fletcher[36], H. Fong[69], J.-D. Fournier[52], S. Franco[23], S. Frasca[28,79], F. Frasconi[19], Z. Frei[53], A. Freise[44], R. Frey[58], V. Frey[23], T. T. Fricke[8], P. Fritschel[10], V. V. Frolov[6], P. Fulda[5], M. Fyffe[6], H. A. G. Gabbard[21], J. R. Gair[94], L. Gammaitoni[32,33], S. G. Gaonkar[14], F. Garufi[4,67], A. Gatto[30], G. Gaur[95,96], N. Gehrels[68], G. Gemme[46], B. Gendre[52], E. Genin[34], A. Gennai[19], J. George[47], L. Gergely[97], V. Germain[7], Archisman Ghosh[15], S. Ghosh[9,51], J. A. Giaime[2,6], K. D. Giardina[6], A. Giazotto[19], K. Gill[98], A. Glaefke[36], E. Goetz[99], R. Goetz[5], L. Gondan[53], G. González[2], J. M. Gonzalez Castro[18,19], A. Gopakumar[100], N. A. Gordon[36], M. L. Gorodetsky[48], S. E. Gossan[1], M. Gosselin[34], R. Gouaty[7], C. Graef[36], P. B. Graff[62], M. Granata[65], A. Grant[36], S. Gras[10], C. Gray[37], G. Greco[56,57], A. C. Green[44], P. Groot[51], H. Grote[8], S. Grunewald[29], G. M. Guidi[56,57], X. Guo[70], A. Gupta[14], M. K. Gupta[96], K. E. Gushwa[1], E. K. Gustafson[1], R. Gustafson[99], J. J. Hacker[22], B. R. Hall[55], E. D. Hall[1], G. Hammond[36], M. Haney[100], M. M. Hanke[8], J. Hanks[37], C. Hanna[72], M. D. Hannam[92], J. Hanson[6], T. Hardwick[2], J. Harms[56,57], G. M. Harry[101], I. W. Harry[29], M. J. Hart[36], M. T. Hartman[5], C.-J. Haster[44], K. Haughian[36], A. Heidmann[59], M. C. Heintze[5,6], H. Heitmann[52], P. Hello[23], G. Hemming[34], M. Hendry[36], I. S. Heng[36], J. Hennig[36], A. W. Heptonstall[1], M. Heurs[8,17], S. Hild[36], D. Hoak[102], K. A. Hodge[1], D. Hofman[65], S. E. Hollitt[103], K. Holt[6], D. E. Holz[75], P. Hopkins[92], D. J. Hosken[103], J. Hough[36], E. A. Houston[36], E. J. Howell[50], Y. M. Hu[36], S. Huang[73], E. A. Huerta[82,104], D. Huet[23], B. Hughey[98], S. Husa[66], S. H. Huttner[36], T. Huynh-Dinh[6], A. Idrisy[72], N. Indik[8], D. R. Ingram[37], R. Inta[71], H. N. Isa[36], J.-M. Isac[59], M. Isi[1], G. Islas[22], T. Isogai[10], B. R. Iyer[15], K. Izumi[37], T. Jacqmin[59], H. Jang[77], K. Jani[63], P. Jaranowski[105], S. Jawahar[106], F. Jiménez-Forteza[66], W. W. Johnson[2], D. I. Jones[26], R. Jones[36], R. J. G. Jonker[9], L. Ju[50], Haris K[107], C. V. Kalaghatgi[24,92], V. Kalogera[82], S. Kandhasamy[21], G. Kang[77], J. B. Kanner[1], S. Karki[58], M. Kasprzack[2,23,34], E. Katsavounidis[10], W. Katzman[6], S. Kaufer[17], T. Kaur[50], K. Kawabe[37], F. Kawazoe[8,17], F. Kéfélian[52], M. S. Kehl[69], D. Keitel[8,66], D. B. Kelley[35], W. Kells[1], R. Kennedy[86], J. S. Key[85], A. Khalaidovski[8], F. Y. Khalili[48], I. Khan[12], S. Khan[92], Z. Khan[96], E. A. Khazanov[108], N. Kijbunchoo[37], C. Kim[77], J. Kim[109], K. Kim[110], Nam-Gyu Kim[77], Namjun Kim[40], Y.-M. Kim[109], E. J. King[103], P. J. King[37], D. L. Kinzel[6], J. S. Kissel[37], L. Kleybolte[27], S. Klimenko[5], S. M. Koehlenbeck[8], K. Kokeyama[2], S. Koley[9], V. Kondrashov[1], A. Kontos[10], M. Korobko[27], W. Z. Korth[1], I. Kowalska[60], D. B. Kozak[1], V. Kringel[8], B. Krishnan[8], A. Królak[111,112], C. Krueger[17], G. Kuehn[8], P. Kumar[69], L. Kuo[73], A. Kutynia[111], B. D. Lackey[35], M. Landry[37], J. Lange[113], B. Lantz[40], P. D. Lasky[114], A. Lazzarini[1], C. Lazzaro[63,42], P. Leaci[28,29,79], S. Leavey[36], E. O. Lebigot[30,70], C. H. Lee[109], H. K. Lee[110], H. M. Lee[115], K. Lee[36], A. Lenon[35], M. Leonardi[90,91], J. R. Leong[8], N. Leroy[23], N. Letendre[7], Y. Levin[114], B. M. Levine[37], T. G. F. Li[1], A. Libson[10], T. B. Littenberg[116], N. A. Lockerbie[106], J. Logue[36], A. L. Lombardi[102], J. E. Lord[35], M. Lorenzini[12,13], V. Loriette[117], M. Lormand[6], G. Losurdo[57], J. D. Lough[8,17], H. Lück[8,17], A. P. Lundgren[8], J. Luo[78], R. Lynch[10], Y. Ma[50], T. MacDonald[40], B. Machenschalk[8], M. MacInnis[10], D. M. Macleod[2], F. Magaña-Sandoval[35], R. M. Magee[55], M. Mageswaran[1],

E. Majorana[28], I. Maksimovic[117], V. Malvezzi[13,25], N. Man[52], I. Mandel[44], V. Mandic[83], V. Mangano[36], G. L. Mansell[20], M. Manske[16], M. Mantovani[34], F. Marchesoni[33,118], F. Marion[7], S. Márka[39], Z. Márka[39], A. S. Markosyan[40], E. Maros[1], F. Martelli[56,57], L. Martellini[52], I. W. Martin[36], R. M. Martin[5], D. V. Martynov[1], J. N. Marx[1], K. Mason[10], A. Masserot[7], T. J. Massinger[35], M. Masso-Reid[36], F. Matichard[10], L. Matone[39], N. Mavalvala[10], N. Mazumder[55], G. Mazzolo[8], R. McCarthy[37], D. E. McClelland[20], S. McCormick[6], S. C. McGuire[119], G. McIntyre[1], J. McIver[1], D. J. McManus[20], S. T. McWilliams[104], D. Meacher[72], G. D. Meadors[8,29], J. Meidam[9], A. Melatos[84], G. Mendell[37], D. Mendoza-Gandara[8], R. A. Mercer[16], E. Merilh[37], M. Merzougui[52], S. Meshkov[1], C. Messenger[36], C. Messick[72], P. M. Meyers[83], F. Mezzani[28,79], H. Miao[44], C. Michel[65], H. Middleton[44], E. E. Mikhailov[120], L. Milano[4,67], J. Miller[10], M. Millhouse[31], Y. Minenkov[13], J. Ming[8,29], S. Mirshekari[121], C. Mishra[15], S. Mitra[14], V. P. Mitrofanov[48], G. Mitselmakher[5], R. Mittleman[10], A. Moggi[19], M. Mohan[34], S. R. P. Mohapatra[10], M. Montani[56,57], B. C. Moore[89], C. J. Moore[122], D. Moraru[37], G. Moreno[37], S. R. Morriss[85], K. Mossavi[8], B. Mours[7], C. M. Mow-Lowry[44], C. L. Mueller[5], G. Mueller[5], A. W. Muir[92], Arunava Mukherjee[15], D. Mukherjee[16], S. Mukherjee[85], N. Mukund[14], A. Mullavey[6], J. Munch[103], D. J. Murphy[39], P. G. Murray[36], A. Mytidis[5], I. Nardecchia[13,25], L. Naticchioni[28,79], R. K. Nayak[123], V. Necula[5], K. Nedkova[102], G. Nelemans[9,51], M. Neri[45,46], A. Neunzert[99], G. Newton[36], T. T. Nguyen[20], A. B. Nielsen[8], S. Nissanke[9,51], A. Nitz[8], F. Nocera[34], D. Nolting[6], M. E. Normandin[85], L. K. Nuttall[35], J. Oberling[37], E. Ochsner[16], J. O'Dell[124], E. Oelker[10], G. H. Ogin[125], J. J. Oh[126], S. H. Oh[126], F. Ohme[92], M. Oliver[66], P. Oppermann[8], Richard J. Oram[6], B. O'Reilly[6], R. O'Shaughnessy[113], D. J. Ottaway[103], R. S. Ottens[5], H. Overmier[6], B. J. Owen[71], A. Pai[107], S. A. Pai[47], J. R. Palamos[58], O. Palashov[108], C. Palomba[28], A. Pal-Singh[27], H. Pan[73], C. Pankow[82], F. Pannarale[92], B. C. Pant[47], F. Paoletti[19,34], A. Paoli[34], M. A. Papa[8,16,29], H. R. Paris[40], W. Parker[6], D. Pascucci[36], A. Pasqualetti[34], R. Passaquieti[18,19], D. Passuello[19], B. Patricelli[18,19], Z. Patrick[40], B. L. Pearlstone[36], M. Pedraza[1], R. Pedurand[65], L. Pekowsky[35], A. Pele[6], S. Penn[127], A. Perreca[1], M. Phelps[36], O. Piccinni[28,79], M. Pichot[52], F. Piergiovanni[56,57], V. Pierro[87,88], G. Pillant[34], L. Pinard[65], I. M. Pinto[87,88], M. Pitkin[36], R. Poggiani[18,19], P. Popolizio[34], E. K. Porter[30], A. Post[8], J. Powell[36], J. Prasad[14], V. Predoi[92], S. S. Premachandra[114], T. Prestegard[83], L. R. Price[1], M. Prijatelj[34], M. Principe[87,88], S. Privitera[29], G. A. Prodi[90,91], L. Prokhorov[48], O. Puncken[8], M. Punturo[33], P. Puppo[28], M. Pürrer[29], H. Qi[16], J. Qin[50], V. Quetschke[85], E. A. Quintero[1], R. Quitzow-James[58], F. J. Raab[37], D. S. Rabeling[20], H. Radkins[37], P. Raffai[53], S. Raja[47], M. Rakhmanov[85], P. Rapagnani[28,79], V. Raymond[29], M. Razzano[18,19], V. Re[25], J. Read[22], C. M. Reed[37], T. Regimbau[52], L. Rei[46], S. Reid[49], D. H. Reitze[1,5], H. Rew[120], S. D. Reyes[35], F. Ricci[28,79], K. Riles[99], N. A. Robertson[1,36], R. Robie[36], F. Robinet[23], A. Rocchi[13], L. Rolland[7], J. G. Rollins[1], V. J. Roma[58], R. Romano[3,4], G. Romanov[120], J. H. Romie[6], D. Rosińska[43,128], S. Rowan[36], A. Rüdiger[8], P. Ruggi[34], K. Ryan[37], S. Sachdev[1], T. Sadecki[37], L. Sadeghian[16], L. Salconi[34], M. Saleem[107], F. Salemi[8], A. Samajdar[123], L. Sammut[84,114], L. Sampson[82], E. J. Sanchez[1], V. Sandberg[37], B. Sandeen[82], J. R. Sanders[35,99], B. Sassolas[65], B. S. Sathyaprakash[92], P. R. Saulson[35], O. Sauter[99], R. L. Savage[37], A. Sawadsky[17], P. Schale[58], R. Schilling[8,135], J. Schmidt[8], P. Schmidt[1,76], R. Schnabel[27], R. M. S. Schofield[58], A. Schönbeck[27], E. Schreiber[8], D. Schuette[8,17], B. F. Schutz[29,92], J. Scott[36], S. M. Scott[20], D. Sellers[6], A. S. Sengupta[95], D. Sentenac[34], V. Sequino[13,25], A. Sergeev[108], G. Serna[22], Y. Setyawati[9,51], A. Sevigny[37], D. A. Shaddock[20], S. Shah[9,51], M. S. Shahriar[82], M. Shaltev[8], Z. Shao[1], B. Shapiro[40], P. Shawhan[62], A. Sheperd[16], D. H. Shoemaker[10], D. M. Shoemaker[63], K. Siellez[52,63], X. Siemens[16], D. Sigg[37], A. D. Silva[11], D. Simakov[8], A. Singer[1], L. P. Singer[68], A. Singh[8,29], R. Singh[2], A. Singhal[12], A. M. Sintes[66], B. J. J. Slagmolen[20], J. R. Smith[22], N. D. Smith[1], R. J. E. Smith[1], E. J. Son[126], B. Sorazu[36], F. Sorrentino[46], T. Souradeep[14], A. K. Srivastava[96], A. Staley[39], M. Steinke[8], J. Steinlechner[36], S. Steinlechner[36], D. Steinmeyer[8,17], B. C. Stephens[16], S. Stevenson[44], R. Stone[85], K. A. Strain[36], N. Straniero[65], G. Stratta[56,57], N. A. Strauss[78], S. Strigin[48], R. Sturani[121], A. L. Stuver[6], T. Z. Summerscales[129], L. Sun[84], P. J. Sutton[92], B. L. Swinkels[34], M. J. Szczepańczyk[98], M. Tacca[30], D. Talukder[58], D. B. Tanner[5], M. Tápai[97], S. P. Tarabrin[8], A. Taracchini[29], R. Taylor[1], T. Theeg[8], M. P. Thirugnanasambandam[1], E. G. Thomas[44], M. Thomas[6], P. Thomas[37], K. A. Thorne[6], K. S. Thorne[76], E. Thrane[114], S. Tiwari[12], V. Tiwari[92], K. V. Tokmakov[106], C. Tomlinson[86], M. Tonelli[18,19], C. V. Torres[85,136], C. I. Torrie[1], D. Töyrä[44], F. Travasso[32,33], G. Traylor[6], D. Trifirò[21], M. C. Tringali[90,91], L. Trozzo[19,130], M. Tse[10], M. Turconi[52], D. Tuyenbayev[85], D. Ugolini[131], C. S. Unnikrishnan[100], A. L. Urban[16], S. A. Usman[35], H. Vahlbruch[17], G. Vajente[1], G. Valdes[85], M. Vallisneri[76], N. van Bakel[9], M. van Beuzekom[9], J. F. J. van den Brand[9,61], C. Van Den Broeck[9], D. C. Vander-Hyde[22,35], L. van der Schaaf[9], J. V. van Heijningen[9], A. A. van Veggel[36], M. Vardaro[41,42], S. Vass[1], M. Vasúth[38], R. Vaulin[10], A. Vecchio[44], G. Vedovato[42], J. Veitch[44], P. J. Veitch[103], K. Venkateswara[132], D. Verkindt[7], F. Vetrano[56,57], A. Viceré[56,57], S. Vinciguerra[44], D. J. Vine[49], J.-Y. Vinet[52], S. Vitale[10], T. Vo[35], H. Vocca[32,33], C. Vorvick[37], D. Voss[5], W. D. Vousden[44], S. P. Vyatchanin[48], A. R. Wade[20], L. E. Wade[133], M. Wade[133], M. Walker[2], L. Wallace[1], S. Walsh[8,16,29], G. Wang[12], H. Wang[44], M. Wang[44], X. Wang[70], Y. Wang[50], R. L. Ward[20], J. Warner[37], M. Was[7], B. Weaver[37], L.-W. Wei[52], M. Weinert[8], A. J. Weinstein[1], R. Weiss[10], T. Welborn[6], L. Wen[50], P. Wessels[8], T. Westphal[8], K. Wette[8], J. T. Whelan[8,113], D. J. White[86], B. F. Whiting[5], R. D. Williams[1], A. R. Williamson[92], J. L. Willis[134], B. Willke[8,17], M. H. Wimmer[8,17], W. Winkler[8], C. C. Wipf[1], H. Wittel[8,17], G. Woan[36], J. Worden[37], J. L. Wright[36], G. Wu[6], J. Yablon[82], W. Yam[10], H. Yamamoto[1], C. C. Yancey[62], M. J. Yap[20], H. Yu[10], M. Yvert[7], A. Zadrożny[111], L. Zangrando[42], M. Zanolin[98], J.-P. Zendri[42], M. Zevin[82], F. Zhang[10], L. Zhang[1], M. Zhang[120], Y. Zhang[113], C. Zhao[50], M. Zhou[82], Z. Zhou[82], X. J. Zhu[50], M. E. Zucker[1,10], S. E. Zuraw[102], and

J. ZWEIZIG[1]

(LIGO SCIENTIFIC COLLABORATION AND VIRGO COLLABORATION)

[1] LIGO, California Institute of Technology, Pasadena, CA 91125, USA
[2] Louisiana State University, Baton Rouge, LA 70803, USA
[3] Università di Salerno, Fisciano, I-84084 Salerno, Italy
[4] INFN, Sezione di Napoli, Complesso Universitario di Monte S. Angelo, I-80126 Napoli, Italy
[5] University of Florida, Gainesville, FL 32611, USA
[6] LIGO Livingston Observatory, Livingston, LA 70754, USA
[7] Laboratoire d'Annecy-le-Vieux de Physique des Particules (LAPP), Université Savoie Mont Blanc, CNRS/IN2P3, F-74941 Annecy-le-Vieux, France
[8] Albert-Einstein-Institut, Max-Planck-Institut für Gravitationsphysik, D-30167 Hannover, Germany
[9] Nikhef, Science Park, 1098 XG Amsterdam, Netherlands
[10] LIGO, Massachusetts Institute of Technology, Cambridge, MA 02139, USA
[11] Instituto Nacional de Pesquisas Espaciais, 12227-010 São José dos Campos, São Paulo, Brazil
[12] INFN, Gran Sasso Science Institute, I-67100 L'Aquila, Italy
[13] INFN, Sezione di Roma Tor Vergata, I-00133 Roma, Italy
[14] Inter-University Centre for Astronomy and Astrophysics, Pune 411007, India
[15] International Centre for Theoretical Sciences, Tata Institute of Fundamental Research, Bangalore 560012, India
[16] University of Wisconsin-Milwaukee, Milwaukee, WI 53201, USA
[17] Leibniz Universität Hannover, D-30167 Hannover, Germany
[18] Università di Pisa, I-56127 Pisa, Italy
[19] INFN, Sezione di Pisa, I-56127 Pisa, Italy
[20] Australian National University, Canberra, ACT 0200, Australia
[21] The University of Mississippi, University, MS 38677, USA
[22] California State University Fullerton, Fullerton, CA 92831, USA
[23] LAL, Université Paris-Sud, CNRS/IN2P3, Université Paris-Saclay, 91400 Orsay, France
[24] Chennai Mathematical Institute, Chennai 603103, India
[25] Università di Roma Tor Vergata, I-00133 Roma, Italy
[26] University of Southampton, Southampton SO17 1BJ, UK
[27] Universität Hamburg, D-22761 Hamburg, Germany
[28] INFN, Sezione di Roma, I-00185 Roma, Italy
[29] Albert-Einstein-Institut, Max-Planck-Institut für Gravitationsphysik, D-14476 Potsdam-Golm, Germany
[30] APC, AstroParticule et Cosmologie, Université Paris Diderot, CNRS/IN2P3, CEA/Irfu, Observatoire de Paris, Sorbonne Paris Cité,
F-75205 Paris Cedex 13, France
[31] Montana State University, Bozeman, MT 59717, USA
[32] Università di Perugia, I-06123 Perugia, Italy
[33] INFN, Sezione di Perugia, I-06123 Perugia, Italy
[34] European Gravitational Observatory (EGO), I-56021 Cascina, Pisa, Italy
[35] Syracuse University, Syracuse, NY 13244, USA
[36] SUPA, University of Glasgow, Glasgow G12 8QQ, UK
[37] LIGO Hanford Observatory, Richland, WA 99352, USA
[38] Wigner RCP, RMKI, H-1121 Budapest, Konkoly Thege Miklós út 29-33, Hungary
[39] Columbia University, New York, NY 10027, USA
[40] Stanford University, Stanford, CA 94305, USA
[41] Università di Padova, Dipartimento di Fisica e Astronomia, I-35131 Padova, Italy
[42] INFN, Sezione di Padova, I-35131 Padova, Italy
[43] CAMK-PAN, 00-716 Warsaw, Poland
[44] University of Birmingham, Birmingham B15 2TT, UK
[45] Università degli Studi di Genova, I-16146 Genova, Italy
[46] INFN, Sezione di Genova, I-16146 Genova, Italy
[47] RRCAT, Indore MP 452013, India
[48] Faculty of Physics, Lomonosov Moscow State University, Moscow 119991, Russia
[49] SUPA, University of the West of Scotland, Paisley PA1 2BE, UK
[50] University of Western Australia, Crawley, WA 6009, Australia
[51] Department of Astrophysics/IMAPP, Radboud University Nijmegen, P.O. Box 9010, 6500 GL Nijmegen, Netherlands
[52] Artemis, Université Côte d'Azur, CNRS, Observatoire Côte d'Azur, CS F-34229, Nice cedex 4, France
[53] MTA Eötvös University, "Lendulet" Astrophysics Research Group, Budapest 1117, Hungary
[54] Institut de Physique de Rennes, CNRS, Université de Rennes 1, F-35042 Rennes, France
[55] Washington State University, Pullman, WA 99164, USA
[56] Universitá degli Studi di Urbino "Carlo Bo," I-61029 Urbino, Italy
[57] INFN, Sezione di Firenze, I-50019 Sesto Fiorentino, Firenze, Italy
[58] University of Oregon, Eugene, OR 97403, USA
[59] Laboratoire Kastler Brossel, UPMC-Sorbonne Universités, CNRS, ENS-PSL Research University, Collège de France, F-75005 Paris, France
[60] Astronomical Observatory Warsaw University, 00-478 Warsaw, Poland
[61] VU University Amsterdam, 1081 HV Amsterdam, Netherlands
[62] University of Maryland, College Park, MD 20742, USA
[63] Center for Relativistic Astrophysics and School of Physics, Georgia Institute of Technology, Atlanta, GA 30332, USA
[64] Institut Lumière Matière, Université de Lyon, Université Claude Bernard Lyon 1, UMR CNRS 5306, F-69622 Villeurbanne, France
[65] Laboratoire des Matériaux Avancés (LMA), IN2P3/CNRS, Université de Lyon, F-69622 Villeurbanne, Lyon, France
[66] Universitat de les Illes Balears, IAC3—IEEC, E-07122 Palma de Mallorca, Spain
[67] Universitá di Napoli "Federico II," Complesso Universitario di Monte S. Angelo, I-80126 Napoli, Italy
[68] NASA/Goddard Space Flight Center, Greenbelt, MD 20771, USA
[69] Canadian Institute for Theoretical Astrophysics, University of Toronto, Toronto, ON M5S 3H8, Canada
[70] Tsinghua University, Beijing 100084, China
[71] Texas Tech University, Lubbock, TX 79409, USA

[72] The Pennsylvania State University, University Park, PA 16802, USA
[73] National Tsing Hua University, Hsinchu City, 30013 Taiwan
[74] Charles Sturt University, Wagga Wagga, NSW 2678, Australia
[75] University of Chicago, Chicago, IL 60637, USA
[76] Caltech CaRT, Pasadena, CA 91125, USA
[77] Korea Institute of Science and Technology Information, Daejeon 305-806, Korea
[78] Carleton College, Northfield, MN 55057, USA
[79] Universitá di Roma "La Sapienza," I-00185 Roma, Italy
[80] University of Brussels, Brussels B-1050, Belgium
[81] Sonoma State University, Rohnert Park, CA 94928, USA
[82] Northwestern University, Evanston, IL 60208, USA
[83] University of Minnesota, Minneapolis, MN 55455, USA
[84] The University of Melbourne, Parkville, VIC 3010, Australia
[85] The University of Texas Rio Grande Valley, Brownsville, TX 78520, USA
[86] The University of Sheffield, Sheffield S10 2TN, UK
[87] University of Sannio at Benevento, I-82100 Benevento, Italy
[88] INFN, Sezione di Napoli, I-80100 Napoli, Italy
[89] Montclair State University, Montclair, NJ 07043, USA
[90] Università di Trento, Dipartimento di Fisica, I-38123 Povo, Trento, Italy
[91] INFN, Trento Institute for Fundamental Physics and Applications, I-38123 Povo, Trento, Italy
[92] Cardiff University, Cardiff CF24 3AA, UK
[93] National Astronomical Observatory of Japan, 2-21-1 Osawa, Mitaka, Tokyo 181-8588, Japan
[94] School of Mathematics, University of Edinburgh, Edinburgh EH9 3FD, UK
[95] Indian Institute of Technology, Gandhinagar Ahmedabad Gujarat 382424, India
[96] Institute for Plasma Research, Bhat, Gandhinagar 382428, India
[97] University of Szeged, Dóm tér 9, Szeged 6720, Hungary
[98] Embry-Riddle Aeronautical University, Prescott, AZ 86301, USA
[99] University of Michigan, Ann Arbor, MI 48109, USA
[100] Tata Institute of Fundamental Research, Mumbai 400005, India
[101] American University, Washington, DC 20016, USA
[102] University of Massachusetts-Amherst, Amherst, MA 01003, USA
[103] University of Adelaide, Adelaide, SA 5005, Australia
[104] West Virginia University, Morgantown, WV 26506, USA
[105] University of Białystok, 15-424 Białystok, Poland
[106] SUPA, University of Strathclyde, Glasgow G1 1XQ, UK
[107] IISER-TVM, CET Campus, Trivandrum Kerala 695016, India
[108] Institute of Applied Physics, Nizhny Novgorod, 603950, Russia
[109] Pusan National University, Busan 609-735, Korea
[110] Hanyang University, Seoul 133-791, Korea
[111] NCBJ, 05-400 Świerk-Otwock, Poland
[112] IM-PAN, 00-956 Warsaw, Poland
[113] Rochester Institute of Technology, Rochester, NY 14623, USA
[114] Monash University, VIC 3800, Australia
[115] Seoul National University, Seoul 151-742, Korea
[116] University of Alabama in Huntsville, Huntsville, AL 35899, USA
[117] ESPCI, CNRS, F-75005 Paris, France
[118] Università di Camerino, Dipartimento di Fisica, I-62032 Camerino, Italy
[119] Southern University and A&M College, Baton Rouge, LA 70813, USA
[120] College of William and Mary, Williamsburg, VA 23187, USA
[121] Instituto de Física Teórica, University Estadual Paulista/ICTP South American Institute for Fundamental Research, São Paulo SP 01140-070, Brazil
[122] University of Cambridge, Cambridge CB2 1TN, UK
[123] IISER-Kolkata, Mohanpur, West Bengal 741252, India
[124] Rutherford Appleton Laboratory, HSIC, Chilton, Didcot, Oxon OX11 0QX, UK
[125] Whitman College, 345 Boyer Avenue, Walla Walla, WA 99362 USA
[126] National Institute for Mathematical Sciences, Daejeon 305-390, Korea
[127] Hobart and William Smith Colleges, Geneva, NY 14456, USA
[128] Janusz Gil Institute of Astronomy, University of Zielona Góra, 65-265 Zielona Góra, Poland
[129] Andrews University, Berrien Springs, MI 49104, USA
[130] Università di Siena, I-53100 Siena, Italy
[131] Trinity University, San Antonio, TX 78212, USA
[132] University of Washington, Seattle, WA 98195, USA
[133] Kenyon College, Gambier, OH 43022, USA
[134] Abilene Christian University, Abilene, TX 79699, USA
[135] Deceased, 2015 May.
[136] Deceased, 2015 March.